Impact of Simvastatin on Adipose Tissue: Pleiotropic Effects *in Vivo*

Tayeba Khan, Mark P. Hamilton, Dorothy I. Mundy, Streamson C. Chua, and Philipp E. Scherer

Departments of Cell Biology (T.K.) and Medicine (S.C.C.), Diabetes Research Center, Albert Einstein College of Medicine, Bronx, New York 10461; and Touchstone Diabetes Center (M.P.H., D.I.M., P.E.S.), Departments of Internal Medicine and Cell Biology (D.I.M., P.E.S.), University of Texas Southwestern Medical Center, Dallas, Texas 75390

Statins belong to a class of drugs well known for their ability to reduce circulating low-density lipoprotein cholesterol. In addition to cholesterol lowering, they also exhibit potential antiinflammatory and antioxidant properties, suggesting that tissues other than liver may be targeted by statins to exert their beneficial metabolic effects. Adipocytes have received very little attention as a potential target of these drugs, possibly because adipocytes are not a major source of biosynthetic cholesterol. Here, we examine the effects of simvastatin on the secretory pathway, inflammation, and cellular metabolism of adipocytes as well as on whole-body insulin sensitivity. We find that statins have a selective effect on the secretion of the insulin-sensitizing adipokine adiponectin by reducing circulating levels of the high-molecular-weight form of adiponectin specifically with a concomitant increase in intracellular adiponectin levels. However, these effects on adiponectin do not translate into changes in metabolism or whole-body insulin sensitivity, potentially due to additional antiinflammatory properties of statins. In addition, *ob/ob* mice treated with statins have reduced adiposity and an altered ultrastructure of the plasma membrane with respect to caveolar histology. Our data demonstrate that statins have major effects on the cellular physiology of the adipocyte on multiple levels. **(*Endocrinology* 150: 5262–5272, 2009)**

One of the most widely prescribed category of drugs for cholesterol lowering in the United States are 3-hydroxy-3-methylglutaryl coenzyme A (HMG-CoA) reductase inhibitors, more commonly known as statins. Statins function by competitively inhibiting the key rate-limiting step in cholesterol biosynthesis: the conversion of HMG-CoA to mevalonate. Inhibition of cholesterol biosynthesis results in an up-regulation of low-density lipoprotein (LDL) receptors, thereby contributing to reduced circulating levels of LDL-cholesterol (LDL-C). These reductions in circulating LDL-C range from 20–60% and are associated with reduced cardiovascular disease and mortality rates (1, 2). Numerous studies have suggested that the timing and magnitude of the clinical benefits of statins cannot be explained entirely by its lipid-lowering properties. Clinical benefits are often observed within 6 months, before significant regression in atherosclerotic plaques. In the last few years, new insights have been obtained on additional mechanisms of statin action. Other effects of statins may include improvements in endothelial dysfunction, increased nitric oxide bioavailability, antioxidant properties, antiinflammatory properties, and stabilization of atherosclerotic plaques (3, 4). Statins are thought to have additional benefits beyond cardiovascular disease, such as in type 2 diabetes, hypertension, dementia, cancer, and bone metabolism (1). This diversity of effects makes it likely that statins can affect numerous cell types and tissues, either through their lipid-lowering properties or through alternative mechanisms.

The liver is the primary target of statins due to its important role in the regulation of cholesterol biosynthesis and LDL turnover. However, the additional benefits that

ISSN Print 0013-7227 ISSN Online 1945-7170
Printed in U.S.A.

doi: 10.1210/en.2009-0603 Received June 1, 2009. Accepted September 2, 2009.
First Published Online October 9, 2009

Abbreviations: Cav-1, Caveolin-1; FFA, free fatty acid; HMG-CoA, 3-hydroxy-3-methylglutaryl coenzyme A; HMW, high molecular weight; LDL, low-density lipoprotein; LDL-C, LDL-cholesterol; mpk, milligrams per kilogram of weight; SAA-3, serum amyloid A3.

statins display suggest important effects in nonhepatic tissues and cell types as well. Adipose tissue is a good candidate tissue to further explore statin action due to its unique ability for bulk cholesterol storage (5). Although most cell types use cholesterol predominantly to maintain the structure of their cell membrane, adipocytes are unique for their storage capacity of very large quantities of cholesterol, accounting for as much as 25% of whole-body cholesterol. Adipocytes have a relatively low *de novo* cholesterol synthesis rate, accounting for less than 10% of total systemic cholesterol production. Most adipocyte cholesterol is in a free, nonesterified form and is localized to lipid droplets (6). In addition, the adipocyte plasma membrane is extremely rich in lipid raft and caveolar structures. Both rafts and caveolae are microdomains highly enriched in cholesterol and are very sensitive to even modest changes in cellular cholesterol levels.

Although there have been a number of clinical reports indicating that statins have an effect on insulin sensitivity, this is far from being an accepted fact in the field, with almost an equal number of reports arguing against a direct impact on any parameters with respect to carbohydrate metabolism. Much of the variability is likely due to differences in the type of statins used, length of treatment, and/or differences in patient populations. In addition, many studies examine statin effects using *in vitro* models, which are not always an accurate reflection of normal physiological conditions *in vivo*. Therefore, we set out to examine the effects of statins on wild-type and obese mouse models. We chose to use simvastatin, because this is a lipophilic statin, with high rate of absorption, and it also represents one of the more potent statins on the market with respect to LDL-C reductions.

Materials and Methods

Animals

Mice (FVB) were maintained on 12-h light, 12-h dark cycle with *ad libitum* access to water and standard chow diet (no. 5058; Lab-Diet, Richmond, IN) or high-fat diet (no. D12492-60 kcal% fat, Research Diets Inc., New Brunswick, NJ), as indicated. Both the FVB wild-type and FVB *ob/ob* mice were bred in-house. During a high-fat diet challenge, wild-type mice were fed high-fat diet pellets for 4 wk. The colony was maintained in a pathogen-free Association for Assessment and Accreditation of Laboratory Animal Care facility at the Albert Einstein College of Medicine under controlled environment settings (22–25 C, 40–50% humidity). Mice were housed in groups of two to five in filter top cages. All animal experimental protocols were approved by the Institute for Animal Studies of the Albert Einstein College of Medicine or by the Institutional Animal Care and Use Committee of University of Texas Southwestern Medical Center at Dallas.

Statin treatment

Simvastatin was a kind gift from Merck & Co. (Rahway, NJ) and was dissolved in a 0.25% carboxymethylcellulose/PBS solution. Mice were gavaged daily with 40 mg simvastatin/kg body weight. FVB wild-type mice were 8 wk old, and *ob/ob* mice were 4 wk old upon initiation of a 2- to 4-wk statin treatment, as indicated. Tail venous blood was collected before and after initiation of treatment.

Serum analysis and metabolic assays

Glucose was measured by an oxidase-peroxidase assay (Sigma-Aldrich, St. Louis, MO). Insulin and leptin were measured with an insulin and leptin ELISA kit, respectively (Millipore, Billerica, MA). Adiponectin and resistin were measured by RIA (Millipore). Triglycerides (Infinity triglyceride kit; Thermo Electron Corp., Bellefonte, PA) and free fatty acids (FFAs) (NEFA C; Wako Pure Chemical, Richmond, VA) were measured by colorimetric assays. IL-6 was measured with an ELISA kit (R&D Systems, Minneapolis, MN).

Oral glucose tolerance test

Mice were fasted 2 h before administration of glucose (2.5 g/kg body weight) by oral gavage. Tail venous blood was collected and assayed for glucose. Mice were denied access to food during the course of the study.

Triglyceride clearance

Mice were fasted for 2 h and given 15 μl olive oil per gram body weight by oral gavage. Blood was collected at each time point and assayed for triglyceride and FFAs. Mice were denied access to food during the course of the study.

LPS challenge

Mice were injected ip with LPS (Sigma-Aldrich) at a dose of 0.1 mg/kg body weight. For the LPS challenge time course, blood was collected and assayed for IL-6 (R&D Systems) and serum amyloid A3 (SAA-3). SAA-3 levels were determined by Western blot analysis of 2 μl serum with a polyclonal anti-SAA-3 antibody. For examination of adipose-specific inflammation in response to LPS, mice were killed 90 min after LPS injection and tissues were immediately snap-frozen in liquid nitrogen.

β-Agonist test

Fed mice were injected ip with the β3-adrenergic receptor agonist CL 316,243 (Sigma-Aldrich) at a dose of 1 mg/kg body weight. Blood was collected at 0 and 15 min and assayed for FFA and insulin.

Arginine tolerance test

Mice were fasted 16 h and injected ip with arginine (1 mg/g body weight; Sigma-Aldrich). Blood was collected and assayed for insulin.

In vivo insulin signaling

Mice were fasted for 2 h and injected ip with human insulin at a dose of 1U/kg body weight. Mice were killed at 0, 5, or 10 min after injection, and tissues were immediately frozen in liquid nitrogen. Tissues were homogenized in RIPA buffer, supplemented with complete protease inhibitor cocktail and phosphatase inhibitor cocktail (Roche, Indianapolis, IN). The protein lysate was directly analyzed by Western blot with anti-phospho-

AKT (Cell Signaling Technology Inc., Beverly, MA) and anti-Akt-1 (Santa Cruz Biotechnology Inc., Santa Cruz, CA). Western blot analysis was done using the LI-COR Odyssey infrared imaging system (LI-COR Biotechnology, Lincoln, NE).

Immunoblot analysis

Adipose tissues were homogenized in TNET buffer lacking Triton X-100 (150 mM NaCl, 5 mM EDTA, 50 mM Tris-HCl, pH 7.5), supplemented with complete protease inhibitor cocktail and phosphatase inhibitor cocktail (Roche). This was followed by low-speed centrifugation (3000 × *g* at 4 C) to remove the fat cake from the top of the tube. Triton X-100 was added to the homogenate for a final concentration of 1%, and the extract was cleared at 20,000 × *g* for 15 min at 4 C and mixed with 2× Laemmli sample buffer. Protein samples were resolved on 4–12% Bis-Tris gels, followed by transfer to BA83 nitrocellulose. Blots were probed with various antibodies, as indicated. The anti-caveolin-1 and anti-insulin receptor-β antibodies were obtained from Santa Cruz Biotechnology. Bound antibodies were detected with IRDye 800-conjugated antirabbit or IRDye 700-conjugated antimouse secondary antibodies (Rockland, Gilbertsville, PA). Membranes were scanned with the LI-COR Odyssey infrared imaging system, and band intensities were quantified with Odyssey version 1.2 software (LI-COR).

Adiponectin complex distribution analysis

In serum

The complex distribution of adiponectin was determined by separating 15 μl mouse serum over a Superdex 200 10/300 GL column (GE Healthcare Bio-Sciences Corp., Piscataway, NJ) using a Biologic Workstation fast-performance liquid chromatography system (Bio-Rad, Hercules, CA). The column was equilibrated in column buffer (25 mM HEPES, 150 mM NaCl, 1 mM $CaCl_2$, pH 8.0), and 0.22-ml fractions were collected. Samples (40 μl) were collected over the entire elution of adiponectin and incubated with 10 μl 5× Laemmli sample buffer, followed by boiling for 5 min. Samples were loaded on a Criterion precast 26-well gel (Bio-Rad) and subjected to immunoblotting using 1:1000 polyclonal anti-adiponectin antibody, followed by incubation with IRDye 800-coupled goat antirabbit secondary antibody (Rockland). The fluorescence signal obtained at 30 kDa was quantified as described above.

In adipose tissue

Intracellular adiponectin complex distribution was determined by velocity sedimentation as previously described (7). Briefly, 200 μg protein lysate was loaded on 5–20% sucrose gradients. After separation, 10 fractions (150 μl) were collected and resolved by SDS-PAGE and quantitative Western blotting. Intracellular total adiponectin levels were determined by quantitative Western blotting of the protein lysate used in the complex distribution analysis.

Quantitation of complexes

For each Western blot, the band intensities of each fraction were plotted onto an x-y line graph. The area under the curve for each distinct peak of the high-molecular-weight (HMW), low-molecular-weight, and trimer form was determined. To calculate the percentage of each complex, the area of each complex was divided by the total area under the curve and multiplied by 100.

Half-life determination of adiponectin

Adiponectin was produced as previously described (7, 8). Fractions containing HMW adiponectin complexes were pooled for further processing. Mouse IgGs were purchased from Sigma-Aldrich. HMW adiponectin and IgG were derivatized with the IRDye 800CW and IRDye 700CW N-hydroxysuccinimide ester dyes, respectively, at a dye to protein 1:1 molar ratio according to the manufacturer's instructions (LI-COR). The labeled HMW adiponectin was administered to mice by retroorbital injection at a dose of 0.3 μg/g body weight. Blood was collected 5, 30, 60, and 120 min after injection. For analysis of the injected material in plasma, 1 μl plasma was mixed with 19 μl Tris-buffered saline and 5 μl 5× Laemmli buffer. After separation on a 10–20% Tricine gel (Invitrogen, Carlsbad, CA), the labeled proteins were directly visualized on the LI-COR Odyssey infrared imaging system in the 700- and 800-nm channels by scanning the gels directly without transfer to a membrane. The 32-kDa adiponectin and 50- and 25-kDa IgG heavy and light chain bands were quantified with Odyssey version 2.1 software. After scanning, the gel was stained with Coomassie, and the light chain band was quantified as loading control. Half-life of the respective proteins were calculated as ln(2)/k, where k is the decay constant.

Quantitative real-time PCR analysis

Mice were killed, and tissue was immediately harvested and frozen in liquid nitrogen. RNA was extracted from tissue using TRIzol reagent (Invitrogen), followed by RNA isolation with the QIAGEN (Valencia, CA) RNeasy tissue kit. Total RNA (1 μg) was reverse transcribed with Superscript III reverse transcriptase and oligo$(dT)_{20}$ (Invitrogen). Quantitative real-time PCR was done using Sybr Green I master mix and was performed in the Roche LightCycler 480. Primers were designed such that one primer spans an intron to prevent amplification of any contaminating genomic DNA, if present. All PCR were normalized to 18S rRNA, unless otherwise indicated. Relative expression levels were calculated by the $\Delta\Delta$Ct method (9). All primers are listed in supplemental Table 1 (published as supplemental data on The Endocrine Society's Journals Online web site at http://endo.endojournals.org).

Immunohistochemistry and staining procedures

Fresh adipose tissue was fixed in 10% phosphate-buffered formalin overnight. Paraffin wax sections of 5 μm were processed for hematoxylin and eosin staining. ImageJ software was used to measure adipocyte area and is represented as average adipocyte area (micrometers). Adipocyte size was measured from four mice per genotype (>500 cells per genotype). All images were obtained by a Censys cooled CCD camera (Photometrics, Tucson, AZ) on a Zeiss axiophot (Zeiss, Jena, Germany).

Transmission electron microscopy

Fresh adipose tissue was cut into 1-μm^2 pieces and fixed overnight in 2% paraformaldehyde, 2.5% glutaraldehyde in 0.1 M sodium cacodylate buffer. They were postfixed with 1% osmium tetroxide followed by 1% uranyl acetate, dehydrated through a graded series of ethanol, and embedded in LX112 resin (LADD Research Industries, Williston, VT). Ultrathin sections (80 nm) were cut on a Reichert Ultracut UCT, stained with uranyl acetate followed by lead citrate, and viewed on a JEOL 1200EX transmission electron microscope at 80 kV.

Statistical analysis

Results are presented as means ± SE or the mean. Statistical analysis was performed with the Student's *t* test or with two-way ANOVA analysis and subsequent Tukey test using GraphPad Prism 5 (San Diego, CA). Significance was accepted at $P < 0.05$.

Supplemental data

Details methods for adipocyte differentiation in cell culture, measurement of pancreas insulin content, tissue cholesterol and triglyceride content, and calorimetry can be found in the supplemental data.

Results

Statins selectively alter the release of the HMW form of adiponectin

To determine whether exposure to an HMG-CoA reductase inhibitor has an impact on plasma steady-state levels of the adipocyte-derived factor adiponectin, we used a preclinical model that would also give us the ability to manipulate various parameters. We treated wild-type mice with 40-mpk (milligrams per kilogram of body weight) simvastatin for 2 wk and measured total and HMW levels of adiponectin before and after treatment. We found that statins caused a 40% reduction in the HMW form of adiponectin (Fig. 1A, *left*), whereas total adiponectin levels remained unchanged (Fig. 1A, *right*). Therefore, statins caused a redistribution of complexes, *i.e.* a reduction in percentage of HMW levels. The 20-mpk dose also reduced the HMW form but to a lesser degree (data not shown). Therefore, we chose the 40-mpk dose for further study.

To understand the possible causes for this reduction in circulating HMW adiponectin, we examined intracellular levels of adiponectin in adipose tissue. Statin treatment increased the intracellular complex distribution of HMW adiponectin (Fig. 1B, *left*). Because intracellular levels of total adiponectin were also not significantly altered (Fig. 1B, *right*), this indicates an overall increase in intracellular levels of HMW adiponectin. The increase in intracellular HMW adiponectin occurs without a significant effect on adiponectin mRNA levels (Fig. 1C). The net level of a protein in circulation is a reflection of the rate at which the protein is secreted *vs.* the rate of clearance. We therefore examined whether statins have an impact on the half-life of adiponectin in circulation. The clearance rate was determined by following the plasma concentrations of a fluorescently labeled HMW adiponectin in mice and monitoring the rate of fluorescence decay (10). We found that the clearance rate of HMW adiponectin was similar to that in vehicle-treated mice (Fig. 1D). Combined, the reduced levels of circulating HMW adiponectin, increased intracellular HMW adiponectin, and unaffected clearance rate

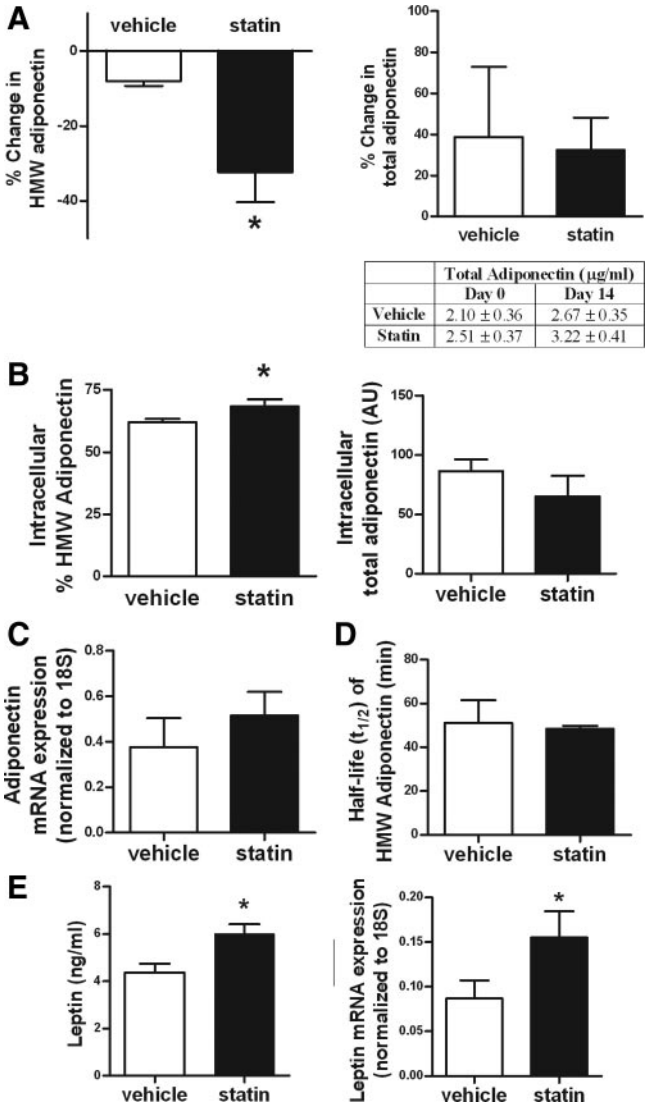

	Total Adiponectin (μg/ml)	
	Day 0	Day 14
Vehicle	2.10 ± 0.36	2.67 ± 0.35
Statin	2.51 ± 0.37	3.22 ± 0.41

FIG. 1. Statin treatment causes a secretion defect of the HMW form of adiponectin. A, The HMW complex of adiponectin (*left*) and total adiponectin (*right*) were measured in 8-wk-old male wild-type mice treated with 40-mpk simvastatin or vehicle daily for 2 wk. Graphs show the percent change in adiponectin levels after treatment. B, The complex distribution of HMW adiponectin (%HMW) and total adiponectin levels were measured intracellularly in epididymal adipose tissue from statin- or vehicle-treated wild-type mice. C, Adiponectin mRNA expression was measured in epididymal adipose tissue by real-time PCR. Expression levels were normalized to 18S rRNA. D, The half-life of HMW adiponectin was measured in statin- or vehicle-treated wild-type mice by iv injecting mice with fluorescently labeled recombinant HMW adiponectin protein and monitoring its rate of decay. E, Circulating leptin protein levels were measured in statin- or vehicle-treated wild-type mice. Leptin mRNA expression was measured in epididymal adipose tissue of statin- or vehicle-treated wild-type mice by real-time PCR. Expression levels were normalized to 18S rRNA. Results are expressed as mean ± SE; n = 5 mice per group. *, $P < 0.05$ by Student's *t* test. AU, Arbitrary units.

of HMW adiponectin all suggest that statins cause a selective secretion defect for HMW adiponectin in adipocytes. In contrast to the effect on HMW adiponectin, statins have no effect on resistin secretion (data not shown). However, leptin secretion is increased, although this in-

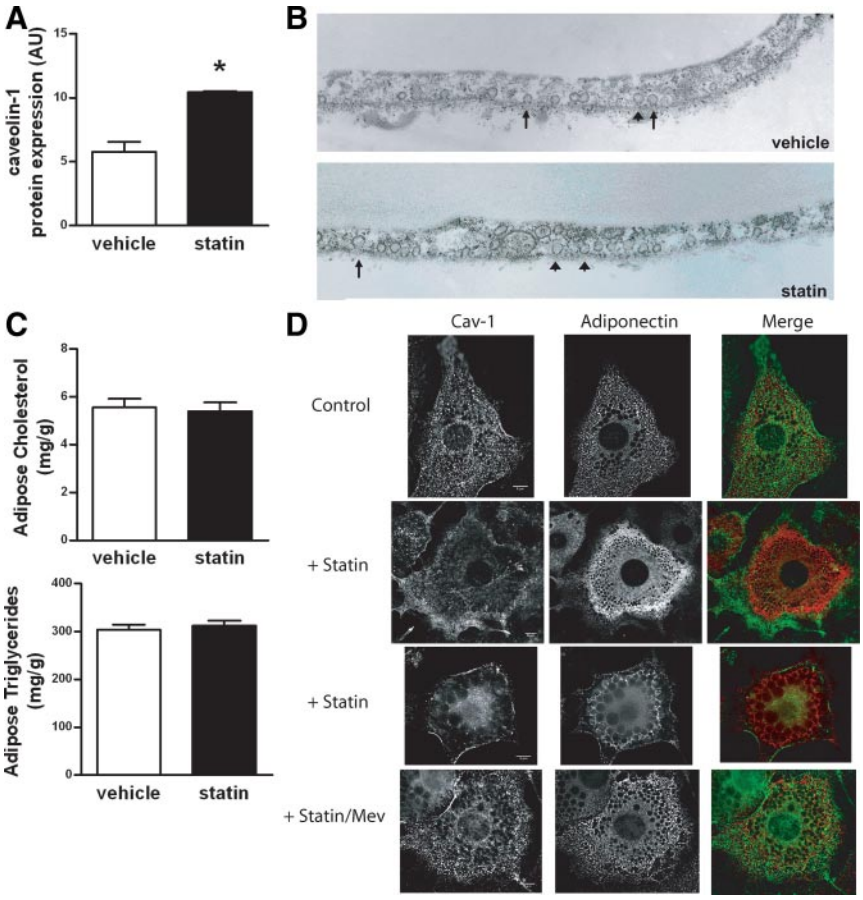

FIG. 2. Caveolae morphology is altered by statin treatment. A, Cav-1 protein expression in epididymal adipose tissue of statin- or vehicle-treated wild-type mice was determined by western blot analysis and band intensity was quantitated with the LI-COR imaging system (mean ± SE; n = 4 mice per group). *, $P < 0.05$ by Student's *t* test. B, Transmission electron microscopy of epididymal adipose tissue of statin- or vehicle-treated mice. The *arrow* indicates a representative invaginated caveola, whereas the *arrowhead* indicates an uninvaginated, vesicle-like caveolar structure. C, Adipocyte cholesterol and triglyceride content were measured in epididymal adipose tissue from statin- or vehicle-treated wild-type mice (mean ± SE; n = 4 mice per group). D, Immunofluorescence staining for cav-1 (*left*) and adiponectin (*middle*) in differentiated 3T3-L1 adipocytes. The two stains were overlaid (*right*). Cav-1 is shown in *green* and adiponectin in *red*. On d 6, 3T3-L1 adipocytes were treated with vehicle (control), 10 μM statin, or 10 μM statin/50 μM mevalonate for 24 h before fixation. The *upper* statin *panel* represents a more frequently occurring distribution, where most adiponectin is intracellular, whereas the *lower* statin *panel* represents a more atypical adipocyte, where most adiponectin is localized to the plasma membrane (n = 3 per treatment).

crease is likely due to an increase in leptin mRNA expression (Fig. 1E).

Caveolae morphology is altered by statin treatment

We noticed that the adiponectin secretion defect caused by statins is reminiscent of the situation seen in cav-1-null (*Cav1KO*) mice. *Cav1KO* mice have reduced circulating levels of total (11) and HMW adiponectin, despite having normal intracellular levels of both total and HMW adiponectin (Wernstedt, I., and P.E. Scherer, manuscript in preparation). It is not surprising that statins have an effect on caveolae, because it is well known that caveolar raft structures are highly sensitive to changes in cholesterol levels. Cellular caveolin-1 (cav-1) and cholesterol levels are proportional to each other, with cav-1 levels increasing at higher levels of cholesterol (12). Statin treatment in other cell types can reduce cav-1 levels in addition to cholesterol levels. Surprisingly, our statin-treated mice had an almost 2-fold increase in cav-1 protein levels in adipose tissue (Fig. 2A). To follow this up at the ultrastructural level, we performed a detailed examination of caveolar structures in adipocytes by visualizing the plasma membrane by transmission electron microscopy (Fig. 2B). Caveolae typically occur as flask-shaped invaginations of the plasma membrane, although they can also occasionally be found as vesicular structures near the plasma membrane. Transmission electron microscopy reveals that statin treatment does in fact increase the number of caveolae. However, there are fewer invaginated caveolae visible, with the majority of the caveolar structures present as vesicular structures immediately adjacent to the plasma membrane. These effects may be caused by a reduction in endogenous cholesterol synthesis early in the secretory pathway in adipocytes that is locally important in the endoplasmic reticulum but accounts only for a small percentage of total cellular cholesterol. Measurements of cholesterol content of adipose tissue after statin treatment does not reveal any effects on total tissue cholesterol or triglyceride content (Fig. 2C).

We took advantage of the clearer cellular morphology that 3T3-L1 adipocytes offer compared with primary adipocytes, due to the much smaller lipid droplet sizes. To test whether statin exposure alters the subcellular distribution of cav-1, we treated 3T3-L1 adipocytes with vehicle, statin, or a combination of statin and mevalonate to relieve the inhibition caused by the statin. We stained the cells for cav-1 and adiponectin (Fig. 2D). Cells treated with vehicle have some cav-1 staining at the plasma membrane as expected, whereas there is also significant intracellular staining. Adiponectin antibodies stain predominantly intracellular compartments, with the bulk of the stain corresponding to the endoplasmic reticulum. Upon statin exposure, neither the cav-1 signal nor

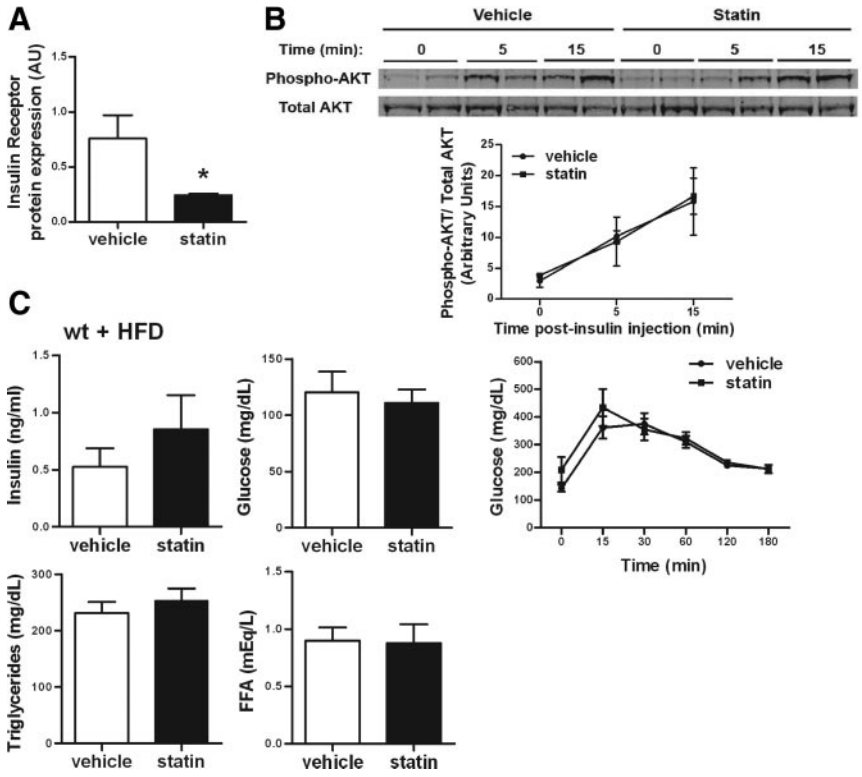

FIG. 3. Statins do not affect insulin sensitivity or other metabolic parameters in adipose tissue. A, Insulin receptor-β protein expression in epididymal adipose tissue of statin- or vehicle-treated wild-type mice after a 4-wk high-fat diet challenge. Protein lysates were analyzed by Western blot analysis with a specific insulin receptor-β antibody, and band intensity was quantitated with the LI-COR imaging system (mean $\pm$ SE; n = 4 mice per group). B, Insulin signaling in statin- or vehicle-treated wild-type mice during a high-fat diet challenge (4 wk). Mice were injected with 1 U insulin/kg body weight, and epididymal adipose tissue was collected 0, 5, and 15 min after injection. The phosphorylation state of AKT was determined by Western blotting directly with specific antibodies for phospho-AKT and total AKT levels. Band intensities were quantitated as in A (mean $\pm$ SE; n = 3 mice per group). C, Basal levels of circulating insulin, glucose, triglycerides, and FFAs were measured in wild-type mice on 4 wk high-fat diet after a 2-h fast. Glucose levels during an oral glucose tolerance test are shown in the *right panel* (mean $\pm$ SE; n = 5 mice per group). *, $P < 0.05$ by Student's *t* test. AU, Arbitrary units; mEq, milliequivalents.

the adiponectin distribution were significantly affected and remained vastly nonoverlapping (Fig. 2D, *upper* statin *panel*). However, when examining a large number of fields, there were several examples of cells where the adiponectin staining pattern changed and adiponectin is found at or near the plasma membrane (Fig. 2D, *lower* statin *panel*). Although it is not possible to quantify this phenomenon because it is not seen in every cell, it is clear that the adiponectin found at the plasma membrane is not located in caveolae because there was little overlap between the two staining patterns. This point is made more clearly in supplemental movies 1 and 2 that moves the plain of focus along the z-axis for a control or statin-treated adipocyte and demonstrates that adiponectin and cav-1 do not colocalize at any level. Coincubation of cells with statins and mevalonate (which reconstitutes endogenous cholesterol biosynthesis) looks like vehicle-treated controls (Fig. 2D, *bottom*). We conclude that even though statins have an impact on both caveolar structures and HMW adiponectin secretion, we find little physical colocalization of cav-1 and adiponectin.

Statins have no effect on insulin sensitivity

Caveolar raft structures play an important role as docking sites for many signaling proteins. The insulin receptor has previously been shown to reside in rafts and critically depends on the integrity of raft structures in adipocytes for its stability (13). We therefore tested whether the presence of statins has an impact on the insulin sensitivity of mice. Statin treatment of mice on a high-fat diet causes an approximately 75% reduction in insulin receptor expression in adipose tissue (Fig. 3A). This is consistent with the local depletion of cholesterol, which then has an impact on the stability of the insulin receptor. However, even though the insulin receptor is reduced to a significant extent in adipose tissue, this does not translate into any differences at the level of insulin signaling (Fig. 3B). After injection of mice with insulin, we monitored the activation of AKT/protein kinase B, a critical downstream mediator of insulin signaling. AKT activation is similar between vehicle- and statin-treated mice. This is consistent with the suggestion that as little as 10% of total cellular insulin receptors are required to get activated to get a full insulin response, provided that the intracellular signal transduction components are in place and are not negatively affected (14). In line with the absence of an impact on cellular insulin sensitivity in adipocytes, we also failed to detect a difference in systemic insulin sensitivity. Basal insulin and glucose, as well as basal triglyceride and FFA levels, do not display any significant differences (Fig. 3C). Glucose clearance in wild-type mice during unchallenged conditions (data not shown) or a high-fat diet challenge also do not reveal any differences upon exposure of the mice to statins (Fig. 3C). These findings in rodents are therefore consistent with the clinical data available for statin treatment that fail to detect a significant improvement or deterioration in insulin sensitivity.

Studies have shown that *cav1KO* mice have a reduced lipolytic response in response to a β3-receptor agonist

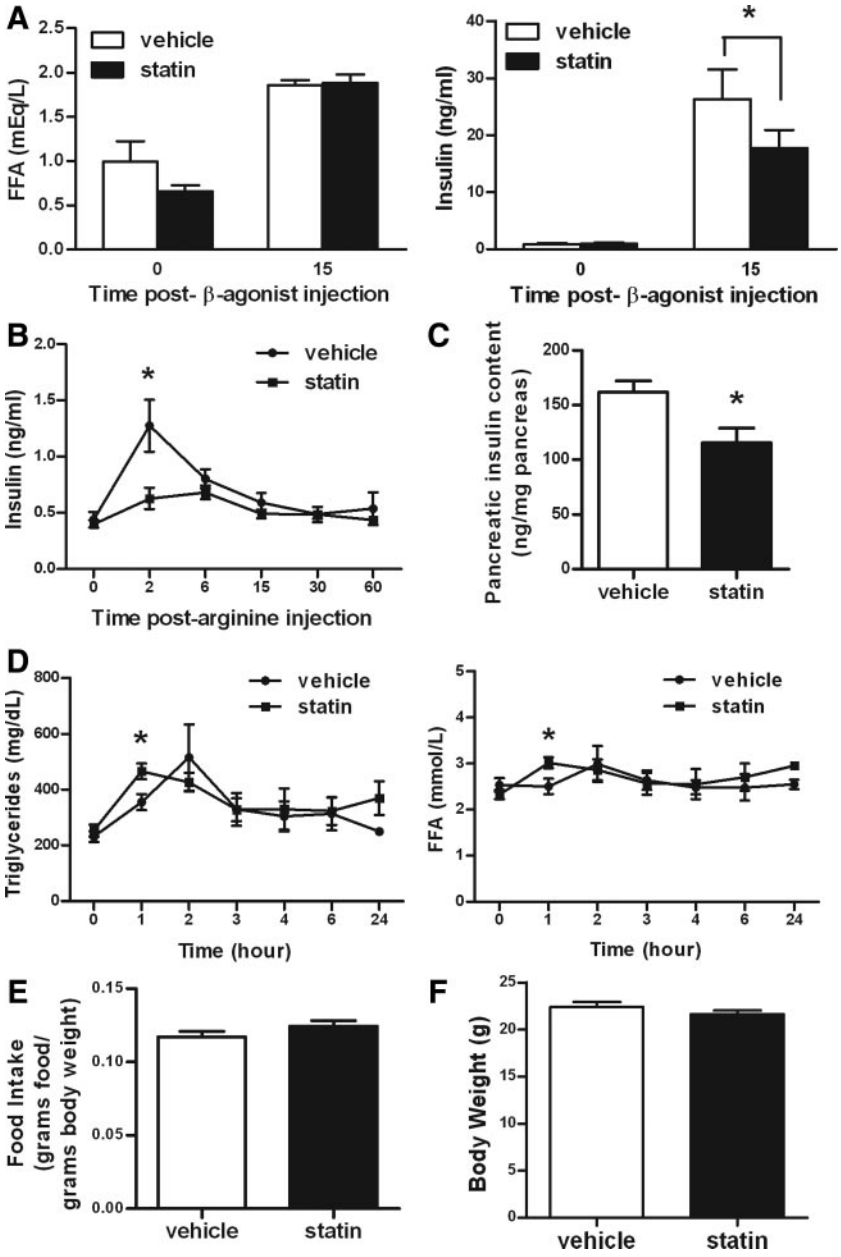

FIG. 4. Statin effects on insulin secretion and lipid metabolism. A, β3-Agonist test in statin- or vehicle-treated wild-type mice. FFA (*left*) and insulin (*right*) levels were measured at 0 and 15 min after injection with the β3-adrenergic receptor agonist CL 316,243 (mean ± SE; n = 5 mice per group). *, $P < 0.05$ by Student's *t* test. B, Arginine tolerance test in statin- or vehicle-treated wild-type mice. Mice were fasted for 16 h and injected with arginine, and insulin levels in circulation were measured (mean ± SE; n = 3 mice per group). *, $P < 0.05$ by two-way ANOVA. C, Pancreatic insulin content was measured in statin- or vehicle-treated wild-type mice (mean ± SE; n = 4 mice per group). *, $P < 0.05$ by Student's *t*-test. D, Serum triglycerides and FFA were measured in statin- or vehicle-treated wild-type mice during a triglyceride challenge (mean ± SE; n = 4 mice per group). *, $P < 0.05$ by two-way ANOVA. E and F, Food intake (E) and body weight (F) were measured in statin- or vehicle-treated wild-type mice and expressed as food intake per grams body weight (mean ± SE; n = 4 mice per group).

(15). Because statins exert a similar effect on adiponectin secretion as does a cav-1-null mutation, we were interested whether the phenotypic similarities extend to lipolysis as well. Upon injection of wild-type mice with β3-agonist, the expected rise in FFA levels can be seen for both vehicle- and statin-treated mice (Fig. 4A, *left*). Furthermore, β3-agonist treatment of white adipocytes can also induce a rapid spike in insulin release at the level of the β-cell (16). This rapid release of insulin can still be observed in statin-treated mice, albeit at a reduced level (Fig. 4A, *right*), indicating a deficiency in white adipocytes, pancreatic β-cells, or a tertiary organ/cell type that is important for this phenomenon. Because arginine acutely stimulates insulin release directly from β-cells, we performed an arginine tolerance test to determine whether insulin content/insulin secretion from the pancreas is affected. Stimulation with arginine indicates a rather strong statin effect, dramatically reducing the first-phase insulin release in response to arginine (Fig. 4B). In addition, measurement of pancreatic insulin content indicates an overall slightly reduced insulin content in statin-treated tissue, even though this effect did not achieve statistical significance (Fig. 4C).

To expand on the metabolic analysis, we also performed an oral triglyceride challenge. Even though triglyceride and FFA induction occurs at an earlier time point in the statin-treated mice, suggesting a possible increased rate of absorption of lipids (Fig. 4D), there is only a limited overall effect. Although we have observed increased circulating levels of leptin by statin treatment (Fig. 1E), this elevation does not have an impact on food intake or body weight of the mice (Fig. 4, E and F). Combined, it is surprising that despite system-wide changes in multiple cell types, there is very little net effect on any of the systemic metabolic parameters measured.

Statin treatment reduces adiposity of *ob*/*ob* mice

To explore the potential impact of statins on obesity, we treated 4-wk-old *ob*/*ob* mice with statins. Similar to the results in wild-type mice (Fig. 3C), statins do not affect systemic insulin sensitivity. Basal levels of insulin, glucose, triglyceride, and FFA, in addition to glucose clearance, are unaffected by statin treatment (Fig. 5A). Interestingly, we observed that the mice in the statin-treated group gained

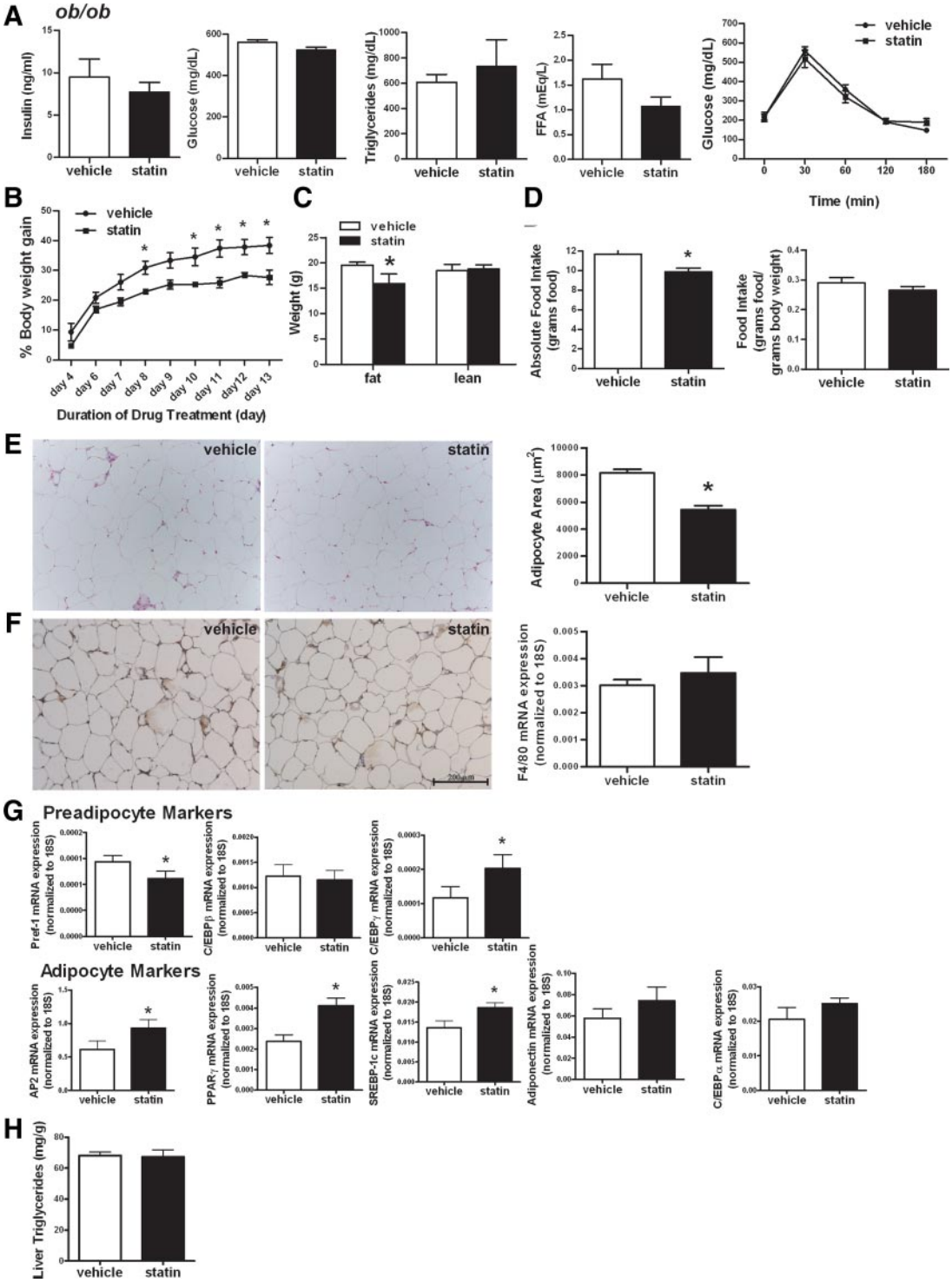

FIG. 5. Statin treatment reduces adiposity of *ob/ob* mice. A, Basal levels of circulating insulin, glucose, triglycerides, and FFAs were measured in vehicle- and statin-treated *ob/ob* mice after a 2-h fast. Glucose levels during an oral glucose tolerance test are shown in the *right panel* (mean ± SE; n = 5 mice per group). B, Body weight was monitored during the course of treatment in 4-wk-old vehicle- or statin- treated *ob/ob* mice. Results are represented as percent body weight gained during the course of the 2-wk treatment period. C, Body composition analysis was determined in *ob/ob* mice at the end of the 2-wk treatment, using magnetic resonance imaging (ECHO MRI). Results indicate fat and lean body mass. D, Food intake was measured during the last week of drug treatment in the *ob/ob* mice. E, Hematoxylin- and eosin-stained sections of epididymal adipose tissue from statin- and vehicle-treated *ob/ob* mice. Quantitation of adipocyte area is shown in the *right panel* (>500 cells counted per group). F, Epididymal adipose tissue sections from statin- and vehicle-treated *ob/ob* mice stained for the macrophage cell surface marker F4/80. F4/80 mRNA expression levels, normalized to 18S rRNA, are shown in the *right panel*. G, Gene expression of several preadipocyte and adipocyte markers were measured in epididymal adipose tissue from statin- and vehicle-treated *ob/ob* mice by real-time PCR. Expression levels were normalized to 18S rRNA. Preadipocyte markers include Pref-1, C/EBPβ, and C/EBPγ; adipocyte markers include adipocyte fatty acid-binding protein (AP2), peroxisome proliferator-activated response (PPARγ), sterol regulatory element binding protein-1C (SREBP-1c), adiponectin, C/EBPα. H, Liver triglyceride content was measured in statin- or vehicle-treated *ob/ob* mice, as described in *Materials and Methods*. Results in B–H are expressed as mean ± SE; n = 4 mice per group. *, $P < 0.05$ by two-way ANOVA (B) and by Student's *t* test (A and C–G).

less weight during the course of treatment compared with the vehicle-treated group (Fig. 5B). Body composition analysis reveals that the difference in body weight is due to a reduction in adipose tissue mass (Fig. 5C). The reduced adiposity in these mice may be due to a reduction in absolute food intake, even though food intake normalized to body weight is unaffected (Fig. 5D). Careful analysis of adipocyte histology reveals that the size of the adipocytes is reduced (Fig. 5E). However, this does not translate into any differences in inflammation of the epididymal (Fig. 5F) or mesenteric (data not shown) adipose tissue depots, as judged by staining for the macrophage cell surface marker F4/80.

There are two possible explanations for this effect on adipocyte size and overall adipose tissue mass. The first possibility is that statins may be anti-adipogenic. There is some *in vitro* evidence for the anti-adipogenic action of statins (17–21), and this may also translate into the *in vivo* setting. An alternative explanation for the reduced adiposity is that statins cause an increase in energy expenditure. Therefore, mice were subject to a metabolic cage study analysis, which demonstrated that statin-treated mice surprisingly have reduced oxygen consumption throughout the light-dark cycle, although there is no change in locomotion (supplemental Fig. S1, A and C). In addition, statin treatment causes a reduction in their respiratory exchange ratio during the day, indicative of a preferential use of fatty acids as an energy source rather than carbohydrates (supplemental Fig. S1B). To test whether the *in vitro* anti-adipogenic effects of statins observed in literature hold up *in vivo*, we examined the expression of several preadipocyte and adipocyte markers. Surprisingly, we found that the preadipocyte marker pref-1 was reduced in adipose tissue from statin-treated mice, whereas the adipocyte markers adipocyte fatty acid-binding protein (aP2), peroxisome proliferator-activated receptor-γ (PPARγ), and sterol regulatory element binding protein-1C (SREBP-1c) were increased (Fig. 5G). These data suggest that adipocyte differentiation *in vivo* may actually be increased by statin treatment. Altered levels of adipogenesis during obesity can trigger adverse metabolic changes in the liver, but statin treatment does not affect hepatic triglyceride levels under these conditions (Fig. 5H).

Statins exert antiinflammatory effects in adipose tissue

In addition to its cholesterol-lowering properties, statins may exert many of their beneficial effects through their antiinflammatory properties. These antiinflammatory properties are predominantly through a direct effect on the liver, as is seen by their ability to reduce systemic levels of the acute-phase reactant protein C-reactive protein (22, 23). We demonstrate here that during a lipopolysaccharide challenge, mice treated with statins display a reduced induction of IL-6 and SAA-3, both of which are inflammatory proteins predominantly secreted by adipose tissue (Fig. 6A). In further support of the concept that statins reduce systemic inflammation via a reduction in adipose-specific inflammation, mRNA levels of IL-6, TNF-α, and SAA-3 are specifically reduced in adipose tissue of statin-treated wild-type mice, whereas their levels are unaffected in the liver (Fig. 6B). These may be direct or indirect effects of statins.

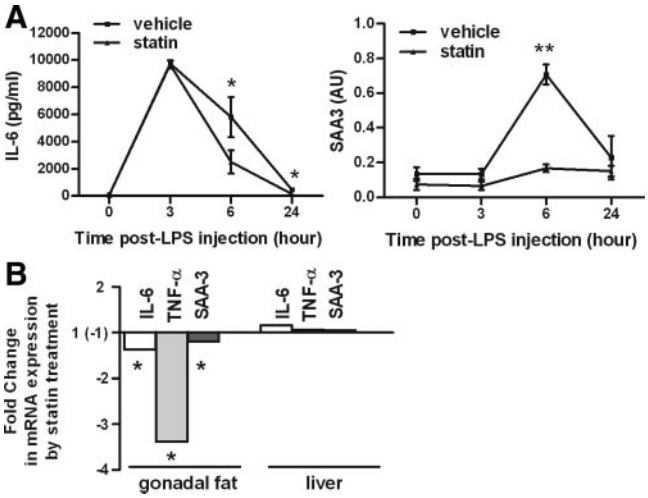

FIG. 6. Statin-treated mice have an attenuated inflammatory response to endotoxin due to reduced inflammation in adipose tissue. A, Statin- or vehicle-treated wild-type mice were injected with lipopolysaccharide (LPS). Circulating levels of IL-6 and SAA-3 were measured 0, 3, 6, and 24 h after LPS injection. B, Inflammatory genes were measured in epididymal adipose tissue and liver by real-time PCR. Expression levels were normalized to 18S rRNA and are represented as fold change in expression of these genes by statin treatment compared with vehicle treatment. Results are expressed as mean ± SE; n = 4 mice per group. *, $P < 0.05$ by two-way ANOVA (A) or Student's *t* test (B).

Discussion

Cholesterol plays a critical role in maintaining the proper function of many different cell types. It is an important structural component of cellular membranes and makes substantial contributions toward maintaining the functional integrity of the cell. The plasma membrane also contains regions with a unique lipid and cholesterol composition, known as lipid rafts and caveolae. Caveolae are distinct from lipid rafts due to their expression of cav proteins, which allows the formation of small, bulb-shaped invaginations of the plasma membrane. Cav-1 and -2 are structural and regulatory components of caveolae and are abundantly expressed in adipocytes. Caveolae are implicated in fatty acid transport and are the docking site for many lipid-linked signaling proteins in adipocytes (12, 24–28). Caveolae are highly susceptible to changes in cho-

lesterol. Rothberg *et al.* (29) demonstrates that exposure of MDCK epithelial cells to cholesterol-binding agents disrupts caveolar structures and that addition of exogenous cholesterol induces caveolae formation. Through the inhibition of cholesterol biosynthesis, statins have also been found to have an inhibitory effect on caveolae formation through reduced cav-1 expression levels (12). Statins have also been shown to reduce membrane cholesterol levels, resulting in significant changes on the lipid composition of the plasma membrane (30).

Our results demonstrate for the first time that statins can also interfere with caveolar formation in adipocytes. Adipocytes from mice treated with simvastatin have a reduced number of the typical bulb-like caveolar structures and have a buildup of caveolar vesicles near the plasma membrane, suggesting a deficiency in membrane docking. *Cav1KO* mice have a complete absence of morphologically distinguishable caveolae in adipocytes. They demonstrate an 80% reduction in circulating levels of total adiponectin and have nearly undetectable amounts of the HMW complex of adiponectin despite normal intracellular levels of total and HMW adiponectin. In addition, the transgenic overexpression of adiponectin in mice (AdipoTG) leads to increased cav-1 levels, indicating a positive relationship between cav-1 and adiponectin expression (31). These data suggest a functional connection between caveolae and adiponectin secretion. A disrupted caveolar structure is also likely to be the mechanism leading to reduced secretion of adiponectin in adipocytes from our statin-treated mice. We demonstrate that the HMW form of adiponectin is increased intracellularly in adipose tissue from statin-treated mice, whereas its levels are reduced in circulation. Clinical studies also support this finding that total adiponectin levels are unaffected by statins (32, 33). Our data suggest that the caveolar structures disrupted by simvastatin have a more specific role in the secretion of HMW adiponectin than for the other isoforms.

There have been several reports indicating that statins have inhibitory effects on adipocyte differentiation (17–20). However, we do not find that simvastatin interferes with adipogenesis *in vivo*. Examination of preadipocyte and adipocyte markers in adipose tissue from statin-treated *ob/ob* mice reveals that simvastatin does not inhibit adipogenesis and, in fact, may even increase adipocyte differentiation. The discrepancy between our study and previous studies likely reflects differences between *in vitro* and *in vivo* experimental settings. In addition, Nakata *et al.* (21) demonstrate that statin-induced inhibition of 3T3-L1 differentiation is more effective earlier in the differentiation process, making this less relevant in an obese mouse model, where adipocytes are predominantly in the fully differentiated state at steady state. An alternative explanation is that the mRNA expression levels of these differentiation markers are not an accurate reflection of their activity levels.

In our current studies, we found that statins have a variety of effects in adipose tissue. We demonstrate that although statins have beneficial effects on inflammation in adipose tissue and reduce adipocyte hypertrophy in *ob/ob* mice, they also have a negative impact on adipose tissue metabolism due to reduced secretion of HMW adiponectin. Combined, these effects result in no net change in insulin sensitivity. However, any effects on inflammation in *ob/ob* mice cannot be separated from effects on body weight, so this could be an indirect effect. It would be interesting to determine whether the differential effects of statins can be linked to distinct physical properties of this class of drugs. The variety of statins on the market today may provide early hints as to how these specific compounds may differ with respect to their absorption and cholesterol-lowering properties and their effects on adipocytes.

Acknowledgments

We thank the members of the Scherer lab for helpful scientific discussion and Drs. John Dietschy and Jay Horton for comments on the manuscript. We also give thanks to Dr. Gary Schwartz for access to the MRI and metabolic cage equipment and to Yuan Xin and Aisha Cordero for technical assistance. We also thank Merck for providing simvastatin for these studies.

Address all correspondence and requests for reprints to: Philipp E. Scherer, Touchstone Diabetes Center, Departments of Internal Medicine and Cell Biology, University of Texas Southwestern Medical Center, 5323 Harry Hines Boulevard, Dallas, Texas 75390-8549. E-mail: Philipp.Scherer@utsouthwestern.edu.

This work was supported by National Institutes of Health Grants R01-DK55758, R24-DK071030-01, and R01-CA112023 (P.E.S.) and by Training Grant T32-DK007513 (Training in Hormone Membrane Interactions) (T.K.).

Disclosure Summary: The authors have nothing to disclose.

References

1. **Rosenson RS** 2008 Lipid lowering with statins. In: Basow DS, ed. UpToDate. Waltham, MA: UpToDate, Inc.
2. **Mills EJ, Rachlis B, Wu P, Devereaux PJ, Arora P, Perri D** 2008 Primary prevention of cardiovascular mortality and events with statin treatments: a network meta-analysis involving more than 65,000 patients. J Am Coll Cardiol 52:1769–1781
3. **Wolfrum S, Jensen KS, Liao JK** 2003 Endothelium-dependent effects of statins. Arterioscler Thromb Vasc Biol 23:729–736
4. **Takemoto M, Liao JK** 2001 Pleiotropic effects of 3-hydroxy-3-methylglutaryl coenzyme A reductase inhibitors. Arterioscler Thromb Vasc Biol 21:1712–17129

5. **Angel A, Farkas J** 1974 Regulation of cholesterol storage in adipose tissue. J Lipid Res 15:491–499
6. **Le Lay S, Ferré P, Dugail I** 2004 Adipocyte cholesterol balance in obesity. Biochem Soc Trans 32:103–106
7. **Pajvani UB, Du X, Combs TP, Berg AH, Rajala MW, Schulthess T, Engel J, Brownlee M, Scherer PE** 2003 Structure-function studies of the adipocyte-secreted hormone Acrp30/adiponectin. Implications for metabolic regulation and bioactivity. J Biol Chem 278:9073–9085
8. **Schraw T, Wang ZV, Halberg N, Hawkins M, Scherer PE** 2008 Plasma adiponectin complexes have distinct biochemical characteristics. Endocrinology 149:2270–2282
9. **Livak KJ, Schmittgen TD** 2001 Analysis of relative gene expression data using real-time quantitative PCR and the $2^{-\Delta\Delta C_T}$ method. Methods 25:402–408
10. **Halberg N, Schraw TD, Wang ZV, Kim JY, Yi J, Hamilton MP, Luby-Phelps K, Scherer PE** 2009 Systemic fate of the adipocyte-derived factor adiponectin. Diabetes 58:1961–1970
11. **Razani B, Combs TP, Wang XB, Frank PG, Park DS, Russell RG, Li M, Tang B, Jelicks LA, Scherer PE, Lisanti MP** 2002 Caveolin-1-deficient mice are lean, resistant to diet-induced obesity, and show hypertriglyceridemia with adipocyte abnormalities. J Biol Chem 277:8635–8647
12. **Feron O, Dessy C, Desager JP, Balligand JL** 2001 Hydroxy-methylglutaryl-coenzyme A reductase inhibition promotes endothelial nitric oxide synthase activation through a decrease in caveolin abundance. Circulation 103:113–118
13. **Cohen AW, Razani B, Wang XB, Combs TP, Williams TM, Scherer PE, Lisanti MP** 2003 Caveolin-1-deficient mice show insulin resistance and defective insulin receptor protein expression in adipose tissue. Am J Physiol Cell Physiol 285:C222–C235
14. **Arsenis G, Hayes GR, Livingston JN** 1985 Insulin receptor cycling and insulin action in the rat adipocyte. J Biol Chem 260:2202–2207
15. **Cohen AW, Razani B, Schubert W, Williams TM, Wang XB, Iyengar P, Brasaemle DL, Scherer PE, Lisanti MP** 2004 Role of caveolin-1 in the modulation of lipolysis and lipid droplet formation. Diabetes 53:1261–1270
16. **Susulic VS, Frederich RC, Lawitts J, Tozzo E, Kahn BB, Harper ME, Himms-Hagen J, Flier JS, Lowell BB** 1995 Targeted disruption of the β3-adrenergic receptor gene. J Biol Chem 270:29483–29492
17. **Tomiyama K, Nishio E, Watanabe Y** 1999 Both wortmannin and simvastatin inhibit the adipogenesis in 3T3-L1 cells during the late phase of differentiation. Jpn J Pharmacol 80:375–378
18. **Nishio E, Tomiyama K, Nakata H, Watanabe Y** 1996 3-Hydroxy-3-methylglutaryl coenzyme A reductase inhibitor impairs cell differentiation in cultured adipogenic cells (3T3-L1). Eur J Pharmacol 301:203–206
19. **Mäuser W, Perwitz N, Meier B, Fasshauer M, Klein J** 2007 Direct adipotropic actions of atorvastatin: differentiation state-dependent induction of apoptosis, modulation of endocrine function, and inhibition of glucose uptake. Eur J Pharmacol 564:37–46
20. **Song C, Guo Z, Ma Q, Chen Z, Liu Z, Jia H, Dang G** 2003 Simvastatin induces osteoblastic differentiation and inhibits adipocytic differentiation in mouse bone marrow stromal cells. Biochem Biophys Res Commun 308:458–462
21. **Nakata M, Nagasaka S, Kusaka I, Matsuoka H, Ishibashi S, Yada T** 2006 Effects of statins on the adipocyte maturation and expression of glucose transporter 4 (SLC2A4): implications in glycaemic control. Diabetologia 49:1881–1892
22. **Ridker PM, Danielson E, Fonseca FA, Genest J, Gotto Jr AM, Kastelein JJ, Koenig W, Libby P, Lorenzatti AJ, MacFadyen JG, Nordestgaard BG, Shepherd J, Willerson JT, Glynn RJ** 2008 Rosuvastatin to prevent vascular events in men and women with elevated C-reactive protein. N Engl J Med 359:2195–2207
23. **Luo Y, Jiang D, Wen D, Yang J, Li L** 2004 Changes in serum interleukin-6 and high-sensitivity C-reactive protein levels in patients with acute coronary syndrome and their responses to simvastatin. Heart Vessels 19:257–262
24. **Pilch PF, Souto RP, Liu L, Jedrychowski MP, Berg EA, Costello CE, Gygi SP** 2007 Cellular spelunking: exploring adipocyte caveolae. J Lipid Res 48:2103–2111
25. **Li S, Okamoto T, Chun M, Sargiacomo M, Casanova JE, Hansen SH, Nishimoto I, Lisanti MP** 1995 Evidence for a regulated interaction between heterotrimeric G proteins and caveolin. J Biol Chem 270:15693–15701
26. **Feron O, Belhassen L, Kobzik L, Smith TW, Kelly RA, Michel T** 1996 Endothelial nitric oxide synthase targeting to caveolae. Specific interactions with caveolin isoforms in cardiac myocytes and endothelial cells. J Biol Chem 271:22810–22814
27. **García-Cardeña G, Oh P, Liu J, Schnitzer JE, Sessa WC** 1996 Targeting of nitric oxide synthase to endothelial cell caveolae via palmitoylation: implications for nitric oxide signaling. Proc Natl Acad Sci USA 93:6448–6453
28. **Song KS, Li Shengwen, Okamoto T, Quilliam LA, Sargiacomo M, Lisanti MP** 1996 Co-purification and direct interaction of Ras with caveolin, an integral membrane protein of caveolae microdomains. Detergent-free purification of caveolae microdomains. J Biol Chem 271:9690–9697
29. **Rothberg KG, Heuser JE, Donzell WC, Ying YS, Glenney JR, Anderson RG** 1992 Caveolin, a protein component of caveolae membrane coats. Cell 68:673–682
30. **Kishida K, Nagaretani H, Kondo H, Kobayashi H, Tanaka S, Maeda N, Nagasawa A, Hibuse T, Ohashi K, Kumada M, Nishizawa H, Okamoto Y, Ouchi N, Maeda K, Kihara S, Funahashi T, Matsuzawa Y** 2003 Disturbed secretion of mutant adiponectin associated with the metabolic syndrome. Biochem Biophys Res Commun 306:286–292
31. **Combs TP, Pajvani UB, Berg AH, Lin Y, Jelicks LA, Laplante M, Nawrocki AR, Rajala MW, Parlow AF, Cheeseboro L, Ding YY, Russell RG, Lindemann D, Hartley A, Baker GR, Obici S, Deshaies Y, Ludgate M, Rossetti L, Scherer PE** 2004 A transgenic mouse with a deletion in the collagenous domain of adiponectin displays elevated circulating adiponectin and improved insulin sensitivity. Endocrinology 145:367–383
32. **Devaraj S, Siegel D, Jialal I** 2007 Simvastatin (40 mg/day), adiponectin levels, and insulin sensitivity in subjects with the metabolic syndrome. Am J Cardiol 100:1397–1399
33. **Kai T, Arima S, Taniyama Y, Nakabou M, Kanamasa K** 2008 Comparison of the effect of lipophilic and hydrophilic statins on serum adiponectin levels in patients with mild hypertension and dyslipidemia: Kinki Adiponectin Interventional (KAI) Study. Clin Exp Hypertens 30:530–540